The 2009 IEEE/RSJ International Conference on
Intelligent Robots and Systems
October 11-15, 2009 St. Louis, USA

Dynamic Force/Torque Equilibrium for Stable Grasping by a Triple Robotic Fingers System

Kenji Tahara, Suguru Arimoto and Morio Yoshida

Abstract— **This paper proposes a stable object grasping method to realize dynamic force/torque equilibrium by using a triple robotic fingers system with soft and deformable hemispherical fingertips. In the authors' previous works, "Blind Grasping" control scheme, which realizes stable object grasping without use of any external sensing such as vision, force, or tactile sensing in the case of using a pair of robot fingers, has been proposed. This control methodology is based on a unique configuration of human hand, called "Fingers-Thumb Opposability". In this paper, a ternary finger in addition to a pair of fingers is introduced not only to expand a stable region of grasping, but also to enhance dexterity and versatility of the multi-fingered robotic hand system. To this end, a "Blind Grasping" manner is modified in order to install it in the triple fingers system. First, dynamics of the triple robotic fingers system and a grasped object with considering rolling constraints is modeled, and a control input based on the blind grasping manner is designed. Next, the closed-loop dynamics is derived and a stability analysis is shown briefly. Finally, its usefulness is discussed through numerical simulation results.**

I. Introduction

A multi-fingered robotic hand system to perform dexterous manipulation tasks like human has been one of the most attractive topics in the field of developing anthropomorphic robotic devices so far. However, it is still now hard to realize a human-like robotic hand system in the functional sense. So far, many works related to the object grasping have been reported [1–5]. Especially, a model for object grasping with rolling constraints has been treated in several works [7–9] since Montana had presented one of the rigid rolling constraint models [6]. In these previous works, modeling and analysis of object grasping have been investigated mainly from the kinematic viewpoint. Also object grasping controllers have mostly been designed based on the inverse dynamics. Therefore, they need the knowledge of an object mass center's location in advance, and the exact information of contact points' locations between the grasped object and each fingertip in realtime. In other words, they need not treat the problem of stability and convergence for closed-loop dynamics explicitly under such a strong assumpition

This work was partially supported by Japan Society for the Promotion of Science (JSPS), Grant-in-Aid for Scientific Research (B) (20360117) and "the Kyushu University Research Superstar Program (SSP)", based on the budget of Kyushu University allocated under President's initiative.

K. Tahara is with the Organization for the Promotion of Advenced Research, Kyushu University, Fukuoka, 819-0395 JAPAN tahara@ieee.org

S. Arimoto is with the Research Organization of Scinece and Engineering, Ritsumeikan University, Kusatsu, 525-8577 JAPAN arimoto@fc.ritsumei.ac.jp

K. Tahara, S. Arimoto and M. Yoshida are with the RIKEN-TRI Collaboration Center for Human-Interactive Robot Research, RIKEN, Nagoya, 463-0003 JAPAN yoshida@nagoya.riken.jp

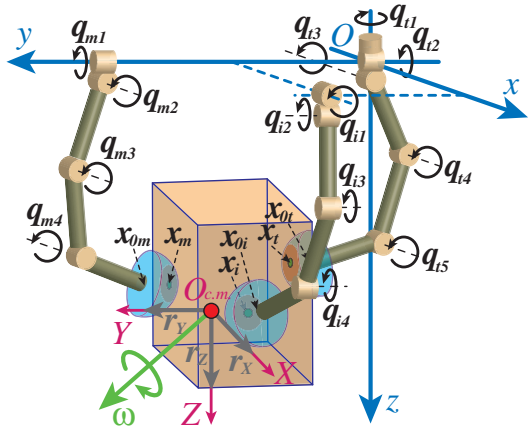

Fig. 1. Triple robotic fingers system

that all the information about the object mass and exact contact point positions is available in realtime. On the other hand, Prattichizzo and Bicchi [10] have treated dynamic analysis of a general manipulation system. Nevertheless, nonholonomic rolling constraints have not yet been taken into consideration explicitly, and it has not mentioned about control design. In recent years, Arimoto *et al.* have proposed one of the dynamic object grasping methods, which need not use any contact point information or object mass information, using a pair of soft robotic fingers with considering rolling constraints [11–13]. Subsequently the authors have improved it and developed a dynamic object manipulation method, called "Blind Grasping" based on their works. This control method is inspired by the unique configuration of human hand, called "Fingers-Thumb Opposability" [14]. Using this controller, stable object grasping is realized not only without use of any external sensing, but also without paying high computational costs such as calculation of inverse dynamics, motion planning according to optimization of certain performance indices, or puzzling about illposedness of inverse kinematics. However, we have assumed that a grasped object does not spin around the opposition axis arising between each contact point on the fingertip during movement so far, because the spinning motion is uncontrollable for a pair of robotic fingers with opposability. In this paper, we introduce a ternary finger in addition to a pair of robotic fingers to take away this strong assupmtion. It is easy to expect that by introducing a surplus finger, a stable region to satisfy the condition of force-torque equlibrium to immobilize the object is larger than the case of a pair of robotic fingers because the number of wrench vectors is increasing. Moreover, it may enhance the dexterity and versatility intuitively. However

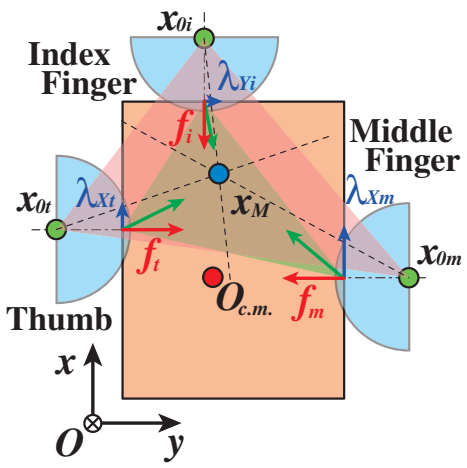

Fig. 2. Centroid $\boldsymbol{x}_M$ of the triangle made by the center of each hemispherical fingertip

in the case of a triple robotic fingers system, especially like our proposed fingers configuration as shown in Fig. 1, each center of contact area between fingertips and the object surfaces makes a triangle, because the ternary finger (now, it is the index finger) is not at the opposite position from any other fingers. This geometrical difference is one of the most remarkable points in the case of a triple robotic fingers system, and thereby the force-torque equiriblium condition to immobilize the object is completely different. Therefore in this paper, we modify the blind grasping control signal to be applicable for our triple robotic fingers system in the following way:

$$\boldsymbol{u}_{sj} = -\frac{f_d}{r_i + r_m + r_t} \boldsymbol{J}_{\boldsymbol{0}j}^{\mathrm{T}} (\boldsymbol{x}_{\boldsymbol{0}j} - \boldsymbol{x}_M) - \boldsymbol{C}_j \dot{\boldsymbol{q}}_j, \quad (1)$$

where $\boldsymbol{x}_{\boldsymbol{0}j}$ denotes each center of hemispherical fingertips, r_j the radius of each fingertip, and $\boldsymbol{x}_M$ the centroid of the triangle made by each center of the hemispherical fingertip as shown in Fig. 2. Apparently, the centroid is given in the following way:

$$\boldsymbol{x}_M = \frac{1}{3} \left(\boldsymbol{x}_{\boldsymbol{0}i} + \boldsymbol{x}_{\boldsymbol{0}m} + \boldsymbol{x}_{\boldsymbol{0}t} \right), \quad (2)$$

where $\dot{\boldsymbol{q}}_j$ denotes each joint angular velocity for each finger, $\boldsymbol{C}_j > 0$ each diagonal positive definite matrix, f_d the nominal desired grasping force, and $\boldsymbol{J}_{\boldsymbol{0}j}$ each Jacobian matrix of each center of the hemispherical fingertips with respect to each joint angular velocity. The subscript of $j = i, m, t$ stands for the *index* finger, *middle* finger, and *thumb* in all equations. Now, let us consider an x-y cross section of our model as shown in Fig. 2. It is well known that in the case of immobilizing a 2-dimensional rectangular parallelepiped object, it needs four frictionless fingers [15]. However in our model, each finger can generate not only a normal grasping force expressed as f_i, f_m, f_t, but also tangential rolling constraint forces expressed as $\lambda_{Y_i}, \lambda_{X_m}, \lambda_{X_t}$ and thereby a force/torque equilibrium to immobilize an object can be established by using these rolling constraint forces even though only three fingers are utilized. It is one of the critically different points compared with grasping by a pair of robotic fingers, and we will show the reason why it can be realized through modeling and analyzing an overall dynamics which includes some physical interaction between each fingertip and a grasped object, and some numerical simulations in this paper.

II. Triple Robotic Fingers System

Let us consider a triple robotic fingers system as shown in Fig. 1. This system is composed of a 4 d.o.f. middle finger and a 5 d.o.f. thumb whose root positions are fixed in an inertial frame and located oppositely to each other, and a 4 d.o.f. index finger whose root position forms an isosceles triangle together with the root positions of other fingers. In other words, the index finger is not at the opposite side from any other fingers. Assume that the grasped object is a rectangular solid, and the shape of each fingertip is hemispheric and made of some soft material such as silicon rubber, and thereby each soft fingertip can make area contact with the object surfaces. In addition, each fingertip can perform rolling without slipping on the object surfaces during movements. Note in this paper that the gravity effect is ignored to have a physical insight into analyzing physical interaction and stability of the system, and to indicate explicitly the difference of the force/torque equilibrium condition between the case of using a pair of robotic fingers and that of using triple robotic fingers. As shown in Fig. 1, symbol O denotes the origin of Cartesian coordinates which commonly regarded as the first, second on third joint center of the thumb. Symbol $O_{c.m.}$ denotes the center of the object mass, and also the origin of object local coordinates. The position of $O_{c.m.}$ in Cartesian coordinates is expressed by $\boldsymbol{x} = (x, y, z)^{\mathrm{T}}$. An instantaneous rotational axis of the object, which is expressed by the object local coodinates $O_{c.m.}$, is $\boldsymbol{\omega} = (\omega_x, \omega_y, \omega_z)^{\mathrm{T}}$ and it means that orientation angular velocities around each axis of $O_{c.m.}$ respectively. Also the position of the center of each contact area in Cartesian coordinates is expressed by $\boldsymbol{x_j}$.

A. Constraints

When each fingertip is rolling on the object surfaces, there arise nonholonomic rolling constraints during movements. These constraint models are derived here. The object orientation in Cartesian coordinates is expressed by the rotational matrix $\boldsymbol{R}$ such that

$$\boldsymbol{R} = \begin{pmatrix} \boldsymbol{r_X} & \boldsymbol{r_Y} & \boldsymbol{r_Z} \end{pmatrix} \in SO(3), \quad (3)$$

where $\boldsymbol{r_X}, \boldsymbol{r_Y}, \boldsymbol{r_Z} \in \mathbb{R}^3$ are mutually orthonormal vectors on the object frame. It is known that this rotational matrix $\boldsymbol{R}$ is one of the members of the group $SO(3)$, and it satisfies the folloing relation

$$\dot{\boldsymbol{R}} = \boldsymbol{R} [\boldsymbol{\omega} \times], \quad [\boldsymbol{\omega} \times] = \begin{pmatrix} 0 & -\omega_z & \omega_y \\ \omega_z & 0 & -\omega_x \\ -\omega_y & \omega_x & 0 \end{pmatrix}, \quad (4)$$

where $\boldsymbol{\omega} = (\omega_x, \omega_y, \omega_z)^{\mathrm{T}}$ is the angular velocity vector for the instantaneous rotational axis of the object expressed by the object local coordinates. Obviously, (4) is not integrable

analytically, and it causes one of the nonholonomic constraints with respect to the angular velocities of the object. On the other hand, the translational velocity of the center of each contact area on the fingertip $\boldsymbol{v_j}$ can be expressed in the following way:

$$\begin{bmatrix} \boldsymbol{v_i} = (r_i - \Delta r_i)\left(-\dot{\boldsymbol{r}}_{\boldsymbol{X}} + \boldsymbol{\Omega}_i \times \boldsymbol{r}_{\boldsymbol{X}}\right) \\ \boldsymbol{v_m} = (r_m - \Delta r_m)\left(-\dot{\boldsymbol{r}}_{\boldsymbol{Y}} + \boldsymbol{\Omega}_m \times \boldsymbol{r}_{\boldsymbol{Y}}\right) \\ \boldsymbol{v_t} = (r_t - \Delta r_t)\left(\dot{\boldsymbol{r}}_{\boldsymbol{Y}} - \boldsymbol{\Omega}_t \times \boldsymbol{r}_{\boldsymbol{Y}}\right), \end{bmatrix} \tag{5}$$

where $\boldsymbol{\Omega_j}$ is the orientation angular velocity vector for each robotic finger at the center of each contact area, and Δr_j is the fingertip's displacement at the center of each contact area such that

$$\begin{bmatrix} \Delta r_i = (r_i + D_i) + \boldsymbol{r}_{\boldsymbol{X}}{}^{\mathrm{T}}(\boldsymbol{x} - \boldsymbol{x}_{\boldsymbol{0}i}) \\ \Delta r_m = (r_m + W_m) + \boldsymbol{r}_{\boldsymbol{Y}}{}^{\mathrm{T}}(\boldsymbol{x} - \boldsymbol{x}_{\boldsymbol{0}m}) \\ \Delta r_t = (r_t + W_t) - \boldsymbol{r}_{\boldsymbol{Y}}{}^{\mathrm{T}}(\boldsymbol{x} - \boldsymbol{x}_{\boldsymbol{0}t}), \end{bmatrix} \tag{6}$$

where D_i is the object depth from the object mass center to the object surface at the index finger's side, and $W_m + W_t$ is the object width. Obviously, $\boldsymbol{v}_j$ is on the tangential plane at the center of each contact area which is the object surface itself in this case. The fingertip's orientation angular velocity vectors $\boldsymbol{\Omega}_j$ can be expressed as a linear homogeneous form with respect to each joint angular velocity such that

$$\boldsymbol{\Omega}_j = \boldsymbol{J}_{\boldsymbol{\Omega}j}\dot{\boldsymbol{q}}_j. \tag{7}$$

The rolling constraints can be expressed in such a way that the velocity of the center of each contact area on the fingertips $\boldsymbol{v_j}$ equals to that on the object surface such that

$$\begin{bmatrix} (r_i - \Delta r_i)\boldsymbol{r}_{\boldsymbol{Y}}{}^{\mathrm{T}}\left(-\dot{\boldsymbol{r}}_{\boldsymbol{X}} + \boldsymbol{\Omega}_i \times \boldsymbol{r}_{\boldsymbol{X}}\right) = \dot{Y}_i \\ (r_i - \Delta r_i)\boldsymbol{r}_{\boldsymbol{Z}}{}^{\mathrm{T}}\left(-\dot{\boldsymbol{r}}_{\boldsymbol{X}} + \boldsymbol{\Omega}_i \times \boldsymbol{r}_{\boldsymbol{X}}\right) = \dot{Z}_i \end{bmatrix} \tag{8}$$

$$\begin{bmatrix} (r_m - \Delta r_m)\boldsymbol{r}_{\boldsymbol{X}}{}^{\mathrm{T}}\left(-\dot{\boldsymbol{r}}_{\boldsymbol{Y}} + \boldsymbol{\Omega}_m \times \boldsymbol{r}_{\boldsymbol{Y}}\right) = \dot{X}_m \\ (r_m - \Delta r_m)\boldsymbol{r}_{\boldsymbol{Z}}{}^{\mathrm{T}}\left(-\dot{\boldsymbol{r}}_{\boldsymbol{Y}} + \boldsymbol{\Omega}_m \times \boldsymbol{r}_{\boldsymbol{Y}}\right) = \dot{Z}_m \end{bmatrix} \tag{9}$$

$$\begin{bmatrix} (r_t - \Delta r_t)\boldsymbol{r}_{\boldsymbol{X}}{}^{\mathrm{T}}\left(\dot{\boldsymbol{r}}_{\boldsymbol{Y}} - \boldsymbol{\Omega}_t \times \boldsymbol{r}_{\boldsymbol{Y}}\right) = \dot{X}_t \\ (r_t - \Delta r_t)\boldsymbol{r}_{\boldsymbol{Z}}{}^{\mathrm{T}}\left(\dot{\boldsymbol{r}}_{\boldsymbol{Y}} - \boldsymbol{\Omega}_t \times \boldsymbol{r}_{\boldsymbol{Y}}\right) = \dot{Z}_t, \end{bmatrix} \tag{10}$$

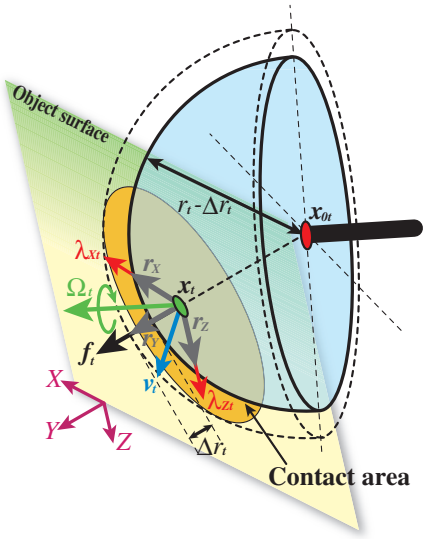

Fig. 3. Contact model at the center of the contact area for the thumb

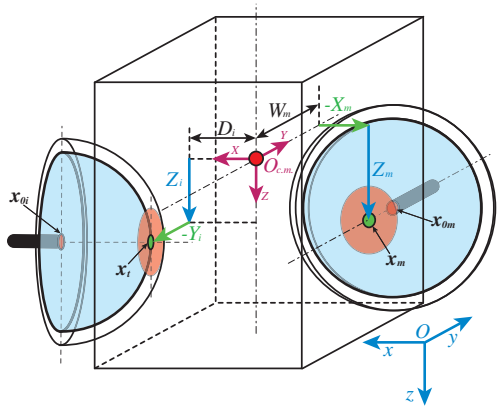

Fig. 4. Projected distances for the index finger (Y_i, Z_i) and the middle finger (X_m, Z_m) on each object surface

where $Y_i, Z_i, X_m, Z_m, X_t, Z_t$ are the projected distances between the object mass center $O_{c.m.}$ and the center of each contact area to X, Y and Z axes of the local frame on the object mass center as shown in Fig. 4. These can be given as follows:

$$\begin{bmatrix} Y_i = -\boldsymbol{r}_{\boldsymbol{Y}}{}^{\mathrm{T}}(\boldsymbol{x} - \boldsymbol{x}_{\boldsymbol{0}i}), & Z_i = -\boldsymbol{r}_{\boldsymbol{Z}}{}^{\mathrm{T}}(\boldsymbol{x} - \boldsymbol{x}_{\boldsymbol{0}i}) \\ X_m = -\boldsymbol{r}_{\boldsymbol{X}}{}^{\mathrm{T}}(\boldsymbol{x} - \boldsymbol{x}_{\boldsymbol{0}m}), & Z_m = -\boldsymbol{r}_{\boldsymbol{Z}}{}^{\mathrm{T}}(\boldsymbol{x} - \boldsymbol{x}_{\boldsymbol{0}m}) \\ X_t = -\boldsymbol{r}_{\boldsymbol{X}}{}^{\mathrm{T}}(\boldsymbol{x} - \boldsymbol{x}_{\boldsymbol{0}t}), & Z_t = -\boldsymbol{r}_{\boldsymbol{Z}}{}^{\mathrm{T}}(\boldsymbol{x} - \boldsymbol{x}_{\boldsymbol{0}t}). \end{bmatrix} \tag{11}$$

Eventually, from (7)∼(11) we obtain

$$\begin{bmatrix} (r_i - \Delta r_i)\left(-\omega_z + \boldsymbol{r}_{\boldsymbol{Z}}{}^{\mathrm{T}}\boldsymbol{J}_{\boldsymbol{\Omega}i}\dot{\boldsymbol{q}}_i\right) = \dot{Y}_i \\ (r_i - \Delta r_i)\left(\omega_y - \boldsymbol{r}_{\boldsymbol{Y}}{}^{\mathrm{T}}\boldsymbol{J}_{\boldsymbol{\Omega}i}\dot{\boldsymbol{q}}_i\right) = \dot{Z}_i \end{bmatrix} \tag{12}$$

$$\begin{bmatrix} (r_m - \Delta r_m)\left(\omega_z - \boldsymbol{r}_{\boldsymbol{Z}}{}^{\mathrm{T}}\boldsymbol{J}_{\boldsymbol{\Omega}m}\dot{\boldsymbol{q}}_m\right) = \dot{X}_m \\ (r_m - \Delta r_m)\left(-\omega_x + \boldsymbol{r}_{\boldsymbol{X}}{}^{\mathrm{T}}\boldsymbol{J}_{\boldsymbol{\Omega}m}\dot{\boldsymbol{q}}_m\right) = \dot{Z}_m \end{bmatrix} \tag{13}$$

$$\begin{bmatrix} (r_t - \Delta r_t)\left(-\omega_z + \boldsymbol{r}_{\boldsymbol{Z}}{}^{\mathrm{T}}\boldsymbol{J}_{\boldsymbol{\Omega}t}\dot{\boldsymbol{q}}_t\right) = \dot{X}_t \\ (r_t - \Delta r_t)\left(\omega_x - \boldsymbol{r}_{\boldsymbol{X}}{}^{\mathrm{T}}\boldsymbol{J}_{\boldsymbol{\Omega}t}\dot{\boldsymbol{q}}_t\right) = \dot{Z}_t, \end{bmatrix} \tag{14}$$

These (12)∼(14) express nonholonomic rolling constraints on the object surfaces, and they are in linear homogeneous with respect to each velocity vector. Therefore, they can be rewritten as Pfaffian constraints which are given as:

$$\begin{bmatrix} \boldsymbol{Y}_{\boldsymbol{q}_i}\dot{\boldsymbol{q}}_i + \boldsymbol{Y}_{\boldsymbol{x}i}\dot{\boldsymbol{x}} + \boldsymbol{Y}_{\boldsymbol{\omega}_i}\boldsymbol{\omega} = 0 \\ \boldsymbol{Z}_{\boldsymbol{q}_i}\dot{\boldsymbol{q}}_i + \boldsymbol{Z}_{\boldsymbol{x}_i}\dot{\boldsymbol{x}} + \boldsymbol{Z}_{\boldsymbol{\omega}_i}\boldsymbol{\omega} = 0 \end{bmatrix} \tag{15}$$

$$\begin{bmatrix} \boldsymbol{X}_{\boldsymbol{q}_m}\dot{\boldsymbol{q}}_m + \boldsymbol{X}_{\boldsymbol{x}m}\dot{\boldsymbol{x}} + \boldsymbol{X}_{\boldsymbol{\omega}m}\boldsymbol{\omega} = 0 \\ \boldsymbol{Z}_{\boldsymbol{q}_m}\dot{\boldsymbol{q}}_m + \boldsymbol{Z}_{\boldsymbol{x}m}\dot{\boldsymbol{x}} + \boldsymbol{Z}_{\boldsymbol{\omega}m}\boldsymbol{\omega} = 0 \end{bmatrix} \tag{16}$$

$$\begin{bmatrix} \boldsymbol{X}_{\boldsymbol{q}_t}\dot{\boldsymbol{q}}_t + \boldsymbol{X}_{\boldsymbol{x}t}\dot{\boldsymbol{x}} + \boldsymbol{X}_{\boldsymbol{\omega}t}\boldsymbol{\omega} = 0 \\ \boldsymbol{Z}_{\boldsymbol{q}_t}\dot{\boldsymbol{q}}_t + \boldsymbol{Z}_{\boldsymbol{x}t}\dot{\boldsymbol{x}} + \boldsymbol{Z}_{\boldsymbol{\omega}t}\boldsymbol{\omega} = 0, \end{bmatrix} \tag{17}$$

where

$$\begin{bmatrix} \boldsymbol{Y}_{\boldsymbol{q}_i} = -(r_i - \Delta r_i)\boldsymbol{r}_{\boldsymbol{Z}}{}^{\mathrm{T}}\boldsymbol{J}_{\boldsymbol{\Omega}i} + \boldsymbol{r}_{\boldsymbol{Y}}{}^{\mathrm{T}}\boldsymbol{J}_{\boldsymbol{0}i}, \\ \boldsymbol{Y}_{\boldsymbol{x}i} = -\boldsymbol{r}_{\boldsymbol{Y}}{}^{\mathrm{T}}, \quad \boldsymbol{Y}_{\boldsymbol{\omega}i} = (Z_i,\ 0,\ -D_i)^{\mathrm{T}} \\ \boldsymbol{Z}_{\boldsymbol{q}_i} = (r_i - \Delta y_i)\boldsymbol{r}_{\boldsymbol{Y}}{}^{\mathrm{T}}\boldsymbol{J}_{\boldsymbol{\Omega}i} + \boldsymbol{r}_{\boldsymbol{Z}}{}^{\mathrm{T}}\boldsymbol{J}_{\boldsymbol{0}i}, \\ \boldsymbol{Z}_{\boldsymbol{x}i} = -\boldsymbol{r}_{\boldsymbol{Z}}{}^{\mathrm{T}}, \quad \boldsymbol{Z}_{\boldsymbol{\omega}i} = (-Y_i,\ D_i,\ 0)^{\mathrm{T}} \end{bmatrix} \tag{18}$$

$$\begin{bmatrix} \boldsymbol{X}_{\boldsymbol{q}_m} = (r_m - \Delta r_m)\boldsymbol{r}_{\boldsymbol{Z}}{}^{\mathrm{T}}\boldsymbol{J}_{\boldsymbol{\Omega}m} + \boldsymbol{r}_{\boldsymbol{X}}{}^{\mathrm{T}}\boldsymbol{J}_{\boldsymbol{0}m}, \\ \boldsymbol{X}_{\boldsymbol{x}m} = -\boldsymbol{r}_{\boldsymbol{X}}{}^{\mathrm{T}}, \quad \boldsymbol{X}_{\boldsymbol{\omega}i} = (0,\ -Z_m,\ W_m)^{\mathrm{T}} \\ \boldsymbol{Z}_{\boldsymbol{q}_m} = -(r_m - \Delta r_m)\boldsymbol{r}_{\boldsymbol{X}}{}^{\mathrm{T}}\boldsymbol{J}_{\boldsymbol{\Omega}m} + \boldsymbol{r}_{\boldsymbol{Z}}{}^{\mathrm{T}}\boldsymbol{J}_{\boldsymbol{0}m}, \\ \boldsymbol{Z}_{\boldsymbol{x}m} = -\boldsymbol{r}_{\boldsymbol{Z}}{}^{\mathrm{T}}, \quad \boldsymbol{Z}_{\boldsymbol{\omega}i} = (-W_m,\ X_m,\ 0)^{\mathrm{T}} \end{bmatrix} \tag{19}$$

$$\begin{bmatrix} \boldsymbol{X}_{\boldsymbol{q}_t} = (r_t - \Delta r_t)\boldsymbol{r}_{\boldsymbol{X}}{}^{\mathrm{T}}\boldsymbol{J}_{\boldsymbol{\Omega}t} + \boldsymbol{r}_{\boldsymbol{Z}}{}^{\mathrm{T}}\boldsymbol{J}_{\boldsymbol{0}t}, \\ \boldsymbol{X}_{\boldsymbol{x}t} = -\boldsymbol{r}_{\boldsymbol{Y}}{}^{\mathrm{T}}, \quad \boldsymbol{X}_{\boldsymbol{\omega}t} = (0,\ -Z_t,\ -W_t)^{\mathrm{T}} \\ \boldsymbol{Z}_{\boldsymbol{q}_t} = (r_t - \Delta r_t)\boldsymbol{r}_{\boldsymbol{X}}{}^{\mathrm{T}}\boldsymbol{J}_{\boldsymbol{\Omega}t} + \boldsymbol{r}_{\boldsymbol{Z}}{}^{\mathrm{T}}\boldsymbol{J}_{\boldsymbol{0}t}, \\ \boldsymbol{Z}_{\boldsymbol{x}t} = -\boldsymbol{r}_{\boldsymbol{Z}}{}^{\mathrm{T}}, \quad \boldsymbol{Z}_{\boldsymbol{\omega}t} = (W_t,\ X_t,\ 0)^{\mathrm{T}}, \end{bmatrix} \tag{20}$$

and $\boldsymbol{J}_{\mathbf{0}i}$, $\boldsymbol{J}_{\mathbf{0}m} \in \mathbb{R}^{3\times 4}$, $\boldsymbol{J}_{\mathbf{0}t} \in \mathbb{R}^{3\times 5}$ are the Jacobian matrices for each $\boldsymbol{x}_{\mathbf{0}j}$ with respect to each joint angle respectively.

B. Soft Fingertip Model

The lumped-parametrized contact model for the deformation of the fingertip at the center of each contact area which has been proposed by Arimoto *et al.* [11] is used here. This model considers only the deformation of normal direction, and doesn't include that of tangential direction. Namely, we assume that the deformation of tangential direction doesn't occur during manipulation for the sake of simplifying the model construction. The reproducing force $f_j(\Delta r_j)$ at the center of each contact area can be expressed as follows:

$$f_j = \bar{f}_j + \xi_j \Delta\dot{r}_j, \quad \bar{f}_j = k\Delta r_j^2, \tag{21}$$

where k stands for a positive constant and ξ_j is a positive scalar function regarding Δr_j, and these are due to the fingertip's material. In addition to this nonlinear spring-damper model with respect to the normal of each contact surface, we introduce a damping model with respect to twist movements between the fingertips and the object surfaces as the energy dissipation functions in the following way [16]:

$$\left[\begin{array}{l} T_i = \eta_i \|\boldsymbol{r_X}^{\mathrm{T}}(\boldsymbol{R\omega} - \boldsymbol{\Omega}_i)\|^2 \\ T_m = \eta_m \|\boldsymbol{r_Y}^{\mathrm{T}}(\boldsymbol{R\omega} - \boldsymbol{\Omega}_m)\|^2 \\ T_t = \eta_t \|\boldsymbol{r_Y}^{\mathrm{T}}(\boldsymbol{R\omega} - \boldsymbol{\Omega}_t)\|^2, \end{array}\right. \tag{22}$$

where η_j is a positive scalar function with resprect to Δr_j which depend on material characteristics of the fingertips.

C. Overall Dynamics

The total kinetic energy of the overall system is given as:

$$K = \sum_{j=i,m,t} \frac{1}{2}\dot{\boldsymbol{q}}_j^{\mathrm{T}} \boldsymbol{H}_j \dot{\boldsymbol{q}}_j + \frac{1}{2}\dot{\boldsymbol{x}}^{\mathrm{T}} \boldsymbol{M} \dot{\boldsymbol{x}} + \frac{1}{2}\boldsymbol{\omega}^{\mathrm{T}} \boldsymbol{I} \boldsymbol{\omega}, \tag{23}$$

where $\boldsymbol{H}_j$ denotes the inertia matrix for each finger, $\boldsymbol{M} = \mathrm{diag}(m, m, m)$ the mass of the object, and $\boldsymbol{I}$ is the inertia tensor for the object represented by the principal axes of inertia. On the other hand, the total potential energy for the overall system is given as follows:

$$P = \sum_{j=i,m,t} P_{f_j} = \sum_{j=i,m,t} \int_0^{\Delta r_j} \bar{f}_j(\Delta r_j)\mathrm{d}\zeta, \tag{24}$$

where $P_{f_j}(\Delta r_j)$ is the potential energy for each fingertip caused by the deformation of the fingertip. Eventually, Lagrange's equation of motion can be obtained by applying the variational principle in such a way

$$\begin{aligned} &\int_{t_0}^{t_1} \left\{ \delta(K - P) + \sum_{j=i,m,t} \boldsymbol{u}_j^{\mathrm{T}} \delta \boldsymbol{q}_j \right\} \mathrm{d}t = \\ &\int_{t_0}^{t_1} \sum_{j=i,m,t} \left\{ \xi_j \Delta\dot{r}_j \frac{\partial \Delta\dot{r}_j}{\partial \dot{\boldsymbol{\Lambda}}} + \frac{\partial T_j}{\partial \dot{\boldsymbol{\Lambda}}} \right\} \delta\boldsymbol{\Lambda} \mathrm{d}t \\ &+ \int_{t_0}^{t_1} (\boldsymbol{Y}_i^{\mathrm{T}}, \boldsymbol{Z}_i^{\mathrm{T}}, \boldsymbol{X}_m^{\mathrm{T}}, \boldsymbol{Z}_m^{\mathrm{T}}, \boldsymbol{X}_t^{\mathrm{T}}, \boldsymbol{Z}_t^{\mathrm{T}})^{\mathrm{T}} \boldsymbol{\lambda} \delta\boldsymbol{\Lambda} \mathrm{d}t, \end{aligned} \tag{25}$$

where $\dot{\boldsymbol{\Lambda}} = (\dot{\boldsymbol{q}}_i^{\mathrm{T}}, \dot{\boldsymbol{q}}_m^{\mathrm{T}}, \dot{\boldsymbol{q}}_t^{\mathrm{T}}, \dot{\boldsymbol{x}}^{\mathrm{T}}, \boldsymbol{\omega}^{\mathrm{T}})^{\mathrm{T}}$, $\boldsymbol{u}_j$ is the input torque vectors for each finger, and $\boldsymbol{Y}_i = (\boldsymbol{Y}_{\boldsymbol{q}_i}^{\mathrm{T}}, \boldsymbol{Y}_{\boldsymbol{x}_i}^{\mathrm{T}}, \boldsymbol{Y}_{\boldsymbol{\omega}_i}^{\mathrm{T}})^{\mathrm{T}}$, $\boldsymbol{X}_m = (\boldsymbol{X}_{\boldsymbol{q}_m}^{\mathrm{T}}, \boldsymbol{X}_{\boldsymbol{x}_m}^{\mathrm{T}}, \boldsymbol{X}_{\boldsymbol{\omega}_m}^{\mathrm{T}})^{\mathrm{T}}$, $\boldsymbol{X}_t = (\boldsymbol{X}_{\boldsymbol{q}_t}^{\mathrm{T}}, \boldsymbol{X}_{\boldsymbol{x}_t}^{\mathrm{T}}, \boldsymbol{X}_{\boldsymbol{\omega}_t}^{\mathrm{T}})^{\mathrm{T}}$, and $\boldsymbol{Z}_j = (\boldsymbol{Z}_{\boldsymbol{q}_j}^{\mathrm{T}}, \boldsymbol{Z}_{\boldsymbol{x}_j}^{\mathrm{T}}, \boldsymbol{Z}_{\boldsymbol{\omega}_j}^{\mathrm{T}})^{\mathrm{T}}$. In addition, $\boldsymbol{\lambda} = (\boldsymbol{\lambda}_i^{\mathrm{T}}, \boldsymbol{\lambda}_m^{\mathrm{T}}, \boldsymbol{\lambda}_t^{\mathrm{T}})^{\mathrm{T}}$ and $\boldsymbol{\lambda}_i = (\lambda_{Y_i}, \lambda_{Z_i})^{\mathrm{T}}$, $\boldsymbol{\lambda}_m = (\lambda_{X_m}, \lambda_{Z_m})^{\mathrm{T}}$, $\boldsymbol{\lambda}_t = (\lambda_{X_t}, \lambda_{Z_t})^{\mathrm{T}}$ denote Lagrange's multipliers. Eventually, we obtain Lagrange's equation of motion such that

For the triple fingers:

$$\begin{aligned} \boldsymbol{H}_i\ddot{\boldsymbol{q}}_i + \left\{\frac{1}{2}\dot{\boldsymbol{H}}_i + \boldsymbol{S}_i\right\}\dot{\boldsymbol{q}}_i + \frac{\partial T_i^{\mathrm{T}}}{\partial \dot{\boldsymbol{q}}_i} - \boldsymbol{J}_{\mathbf{0}i}^{\mathrm{T}} \boldsymbol{r_X} f_i \\ + (\boldsymbol{Y}_{\boldsymbol{q}_i}^{\mathrm{T}}, \boldsymbol{Z}_{\boldsymbol{q}_i}^{\mathrm{T}})\boldsymbol{\lambda}_i = \boldsymbol{u}_i \end{aligned} \tag{26}$$

$$\begin{aligned} \boldsymbol{H}_m\ddot{\boldsymbol{q}}_m + \left\{\frac{1}{2}\dot{\boldsymbol{H}}_m + \boldsymbol{S}_m\right\}\dot{\boldsymbol{q}}_m + \frac{\partial T_m^{\mathrm{T}}}{\partial \dot{\boldsymbol{q}}_m} - \boldsymbol{J}_{\mathbf{0}m}^{\mathrm{T}} \boldsymbol{r_Y} f_m \\ + (\boldsymbol{X}_{\boldsymbol{q}_m}^{\mathrm{T}}, \boldsymbol{Z}_{\boldsymbol{q}_m}^{\mathrm{T}})\boldsymbol{\lambda}_m = \boldsymbol{u}_m \end{aligned} \tag{27}$$

$$\begin{aligned} \boldsymbol{H}_t\ddot{\boldsymbol{q}}_t + \left\{\frac{1}{2}\dot{\boldsymbol{H}}_t + \boldsymbol{S}_t\right\}\dot{\boldsymbol{q}}_t + \frac{\partial T_t^{\mathrm{T}}}{\partial \dot{\boldsymbol{q}}_t} + \boldsymbol{J}_{\mathbf{0}t}^{\mathrm{T}} \boldsymbol{r_Y} f_t \\ + (\boldsymbol{X}_{\boldsymbol{q}_t}^{\mathrm{T}}, \boldsymbol{Z}_{\boldsymbol{q}_t}^{\mathrm{T}})\boldsymbol{\lambda}_t = \boldsymbol{u}_t \end{aligned} \tag{28}$$

For the object:

$$\begin{aligned} \boldsymbol{M}\ddot{\boldsymbol{x}} + (f_i - \lambda_{X_m} - \lambda_{X_t})\boldsymbol{r_X} + (f_m - f_t - \lambda_{Y_i})\boldsymbol{r_Y} \\ - (\lambda_{Z_i} + \lambda_{Z_m} + \lambda_{Z_t})\boldsymbol{r_Z} = \mathbf{0} \end{aligned} \tag{29}$$

$$\begin{aligned} &\boldsymbol{I}\dot{\boldsymbol{\omega}} + \boldsymbol{\omega} \times \boldsymbol{I}\boldsymbol{\omega} + \sum_{j=i,m,t} \frac{\partial T_j^{\mathrm{T}}}{\partial \boldsymbol{\omega}} \\ &+ \begin{pmatrix} 0 \\ Z_i \\ -Y_i \end{pmatrix} f_i + \begin{pmatrix} -Z_m \\ 0 \\ X_m \end{pmatrix} f_m + \begin{pmatrix} Z_t \\ 0 \\ -X_t \end{pmatrix} f_t \\ &+ \begin{pmatrix} Z_i \\ 0 \\ -D_i \end{pmatrix} \lambda_{Y_i} + \begin{pmatrix} 0 \\ -Z_m \\ W_m \end{pmatrix} \lambda_{X_m} + \begin{pmatrix} 0 \\ -Z_t \\ -W_t \end{pmatrix} \lambda_{X_t} \\ &+ \begin{pmatrix} -Y_i \\ D_i \\ 0 \end{pmatrix} \lambda_{Z_i} + \begin{pmatrix} -W_m \\ X_m \\ 0 \end{pmatrix} \lambda_{Z_m} + \begin{pmatrix} W_t \\ X_t \\ 0 \end{pmatrix} \lambda_{Z_t} = \mathbf{0}, \end{aligned} \tag{30}$$

where $\boldsymbol{S}_j$ and $\boldsymbol{S}$ are skew-symmetric matrices. Now, taking inner product of the input vector $\boldsymbol{U} = (\boldsymbol{u}_i^{\mathrm{T}}, \boldsymbol{u}_m^{\mathrm{T}}, \boldsymbol{u}_t^{\mathrm{T}}, \mathbf{0}^{\mathrm{T}}, \mathbf{0}^{\mathrm{T}})^{\mathrm{T}}$ with the output vector $\dot{\boldsymbol{\Lambda}} = (\dot{\boldsymbol{q}}_i^{\mathrm{T}}, \dot{\boldsymbol{q}}_m^{\mathrm{T}}, \dot{\boldsymbol{q}}_t^{\mathrm{T}}, \dot{\boldsymbol{x}}^{\mathrm{T}}, \boldsymbol{\omega}^{\mathrm{T}})^{\mathrm{T}}$ yeilds

$$\dot{\boldsymbol{\Lambda}}^{\mathrm{T}} \boldsymbol{U} = \frac{\mathrm{d}}{\mathrm{d}t}(K + P) = -\sum_{j=i,m,t} (T_j + \xi\Delta\dot{r}_j^2) \leq 0. \tag{31}$$

This inequality expresses that the input-output pair satisfies the passivity condition [17].

III. Design of External Sensor-Less Grasping Control Signal

Let us design a control signal for stable grasping without use of external sensing. We have already shown the basic idea of our controller in (1) and (2) in Section I. In addition to the control signal, we introduce an adaptive control signal to compensate the grasping force from the surplus finger as follows:

$$\boldsymbol{u}_{\boldsymbol{c}j} = -\frac{r_j f_d}{3(r_i + r_m + r_t)} \boldsymbol{J}_{\boldsymbol{\omega}_j}^{\mathrm{T}} \hat{\boldsymbol{N}}_j, \tag{32}$$

where each $\hat{\boldsymbol{N}}_j$ is updated correspoinding to the following equation such that

$$\frac{\mathrm{d}}{\mathrm{d}t}\hat{\boldsymbol{N}}_j = \frac{r_j f_d}{3(r_i + r_m + r_t)} \boldsymbol{\Gamma}_{\boldsymbol{N}_j}^{-1} \boldsymbol{J}_{\boldsymbol{\omega}_j} \dot{\boldsymbol{q}}_j, \tag{33}$$

and $\boldsymbol{\Gamma}_{\boldsymbol{N}_j}^{-1} = \mathrm{diag}(\gamma_{N_{jx}}^{-1}, \gamma_{N_{jy}}^{-1}, \gamma_{N_{jz}}^{-1}) > \mathbf{0}$ is the adaptive estimation gain for each $\hat{\boldsymbol{N}}_j$. These compensation control terms play a important role to realize stable grasping in the case of this triple fingers system. In the case of frictionless fingers, it needs seven fingers to satisfy the form-closure to immobilize a 3-dimensional rectangular solid object. However, this system has only three fingers. Furthermore, the grasping force from the ternary finger is normal to the grasping forces from other fingers. Therefore, in order to realize force/torque equilibrium to immobilize the object, each finger should generate rolling constraint forces which are partially shown in Fig. 2 as λ_{Y_i}, λ_{X_m}, and λ_{X_t}. These rolling constraint forces at the final state cannot be generated if only using the control signals given as (2), and thereby these compensation control signals are necessary to generate the rolling constraint forces at the final state. Eventually, we design the total control signals to the triple robotic fingers system according to the principle of linear superposition such that

$$\boldsymbol{u}_j = \boldsymbol{u}_{\boldsymbol{s}j} + \boldsymbol{u}_{\boldsymbol{c}j}. \tag{34}$$

It is remarkable that the control inputs given as (34) are composed of only kinematic information, joint angles and angular velocities of the triple fingers system. Substituting these control signals into (26)$\sim$(30) yeilds the overall closed-loop dynamics such that

For the triple fingers:

$$\begin{aligned}
&\boldsymbol{H}_i\ddot{\boldsymbol{q}}_i+\left\{\frac{1}{2}\dot{\boldsymbol{H}}_i+\boldsymbol{S}_i+\boldsymbol{C}_i\right\}\dot{\boldsymbol{q}}_i+\frac{\partial {T_i}^{\mathrm{T}}}{\partial \dot{\boldsymbol{q}}_i}-\boldsymbol{J}_{\boldsymbol{0}i}^{\mathrm{T}}\boldsymbol{r}_{\boldsymbol{X}}\Delta f_i\\
&\quad+(\boldsymbol{Y}_{\boldsymbol{q}_i}^{\mathrm{T}},\boldsymbol{Z}_{\boldsymbol{q}_i}^{\mathrm{T}})\boldsymbol{\Delta\lambda}_i-r_iQ\boldsymbol{\Delta N}_i=\boldsymbol{0} \qquad (35)\\
&\boldsymbol{H}_m\ddot{\boldsymbol{q}}_m+\left\{\frac{1}{2}\dot{\boldsymbol{H}}_m+\boldsymbol{S}_m+\boldsymbol{C}_m\right\}\dot{\boldsymbol{q}}_m+\frac{\partial {T_m}^{\mathrm{T}}}{\partial \dot{\boldsymbol{q}}_m}-\boldsymbol{J}_{\boldsymbol{0}m}^{\mathrm{T}}\boldsymbol{r}_{\boldsymbol{Y}}\Delta f_m\\
&\quad+(\boldsymbol{X}_{\boldsymbol{q}_m}^{\mathrm{T}},\boldsymbol{Z}_{\boldsymbol{q}_m}^{\mathrm{T}})\boldsymbol{\Delta\lambda}_m-r_mQ\boldsymbol{\Delta N}_m=\boldsymbol{0} \qquad (36)\\
&\boldsymbol{H}_t\ddot{\boldsymbol{q}}_t+\left\{\frac{1}{2}\dot{\boldsymbol{H}}_t+\boldsymbol{S}_t+\boldsymbol{C}_t\right\}\dot{\boldsymbol{q}}_t+\frac{\partial {T_t}^{\mathrm{T}}}{\partial \dot{\boldsymbol{q}}_t}+\boldsymbol{J}_{\boldsymbol{0}t}^{\mathrm{T}}\boldsymbol{r}_{\boldsymbol{Y}}\Delta f_t\\
&\quad+(\boldsymbol{X}_{\boldsymbol{q}t}^{\mathrm{T}},\boldsymbol{Z}_{\boldsymbol{q}t}^{\mathrm{T}})\boldsymbol{\Delta\lambda}_t+r_tQ\boldsymbol{\Delta N}_t=\boldsymbol{0} \qquad (37)
\end{aligned}$$

For the object:

$$\begin{aligned}
&\boldsymbol{M}\ddot{\boldsymbol{x}}+(\Delta f_i-\Delta\lambda_{X_m}-\Delta\lambda_{X_t})\boldsymbol{r}_{\boldsymbol{X}}\\
&\qquad+(\Delta f_m-\Delta f_t-\Delta\lambda_{Y_i})\boldsymbol{r}_{\boldsymbol{Y}}\\
&\qquad-(\Delta\lambda_{Z_i}+\Delta\lambda_{Z_m}+\Delta\lambda_{Z_t})\boldsymbol{r}_{\boldsymbol{Z}}=\boldsymbol{0} \qquad (38)
\end{aligned}$$

$$\begin{aligned}
&\boldsymbol{I}\dot{\boldsymbol{\omega}}+\boldsymbol{\omega}\times\boldsymbol{I}\boldsymbol{\omega}+\sum_{j=i,m,t}\frac{\partial {T_j}^{\mathrm{T}}}{\partial\boldsymbol{\omega}}+\begin{pmatrix}S_{\omega_x}\\S_{\omega_y}\\S_{\omega_z}\end{pmatrix}\\
&+\begin{pmatrix}0\\Z_i\\-Y_i\end{pmatrix}\Delta f_i+\begin{pmatrix}-Z_m\\0\\X_m\end{pmatrix}\Delta f_m+\begin{pmatrix}Z_t\\0\\-X_t\end{pmatrix}\Delta f_t\\
&+\begin{pmatrix}Z_i\\0\\-D_i\end{pmatrix}\Delta\lambda_{Y_i}+\begin{pmatrix}0\\-Z_m\\W_m\end{pmatrix}\Delta\lambda_{X_m}+\begin{pmatrix}0\\-Z_t\\-W_t\end{pmatrix}\Delta\lambda_{X_t}\\
&+\begin{pmatrix}-Y_i\\D_i\\0\end{pmatrix}\Delta\lambda_{Z_i}+\begin{pmatrix}-W_m\\X_m\\0\end{pmatrix}\Delta\lambda_{Z_m}+\begin{pmatrix}W_t\\X_t\\0\end{pmatrix}\Delta\lambda_{Z_t}=\boldsymbol{0}, \qquad (39)
\end{aligned}$$

where

$$Q=\frac{f_d}{3(r_i+r_m+r_t)} \tag{40}$$

$$\boldsymbol{\Delta N}_j=\boldsymbol{J}_{\boldsymbol{\omega}_j}^{\mathrm{T}}(\hat{\boldsymbol{N}}_j-\boldsymbol{N}_j) \tag{41}$$

$$\begin{cases}
\boldsymbol{N}_i=\dfrac{r_i-\Delta r_i}{r_i}\left(\boldsymbol{r}_{\boldsymbol{Y}}I_Z-\boldsymbol{r}_{\boldsymbol{Z}}I_Y\right)\\
\boldsymbol{N}_m=\dfrac{r_m-\Delta r_m}{r_m}\left(\boldsymbol{r}_{\boldsymbol{Z}}M_X-\boldsymbol{r}_{\boldsymbol{X}}M_Z\right)\\
\boldsymbol{N}_t=\dfrac{r_t-\Delta r_t}{r_t}\left(\boldsymbol{r}_{\boldsymbol{Z}}T_X-\boldsymbol{r}_{\boldsymbol{X}}T_Z\right),
\end{cases}$$

and

$$\begin{cases}
\Delta f_i=f_i-Q\cdot I_X, & \Delta f_m=f_m-Q\cdot M_Y\\
\Delta f_t=f_t-Q\cdot T_Y, & \Delta\lambda_{Y_i}=\lambda_{Y_i}+Q\cdot I_Y\\
\Delta\lambda_{X_m}=\lambda_{X_m}+Q\cdot M_X, & \Delta\lambda_{X_t}=\lambda_{X_t}+Q\cdot T_X\\
\Delta\lambda_{Z_i}=\lambda_{Z_i}+Q\cdot I_Z, & \Delta\lambda_{Z_m}=\lambda_{Z_m}+Q\cdot M_Z\\
\Delta\lambda_{Z_t}=\lambda_{Z_t}+Q\cdot T_Z,
\end{cases} \tag{42}$$

$$\begin{cases}
I_X=2R_i-X_m-X_t\\
I_Y=2Y_i-R_m+R_t\\
I_Z=2Z_i-Z_m-Z_t
\end{cases},\quad
\begin{cases}
M_X=2X_m-R_i-X_t\\
M_Y=2R_m-Y_i+R_t\\
M_Z=2Z_m-Z_i-Z_t
\end{cases}$$
$$\begin{cases}
T_X=2X_t-R_i-X_m\\
T_Y=2R_t+Y_i+R_m\\
T_Z=2Z_t-Z_i-Z_m
\end{cases},\quad
\begin{cases}
R_i=r_i-\Delta r_i+D_i\\
R_m=r_m-\Delta r_m+W_m\\
R_t=r_t-\Delta r_t+W_t
\end{cases} \tag{43}$$

$$\begin{cases}
S_{\omega_x}=Q\{-(r_m-\Delta r_m)M_Z+(r_t-\Delta r_t)T_Z\}\\
S_{\omega_y}=Q(r_i-\Delta r_i)I_Z\\
S_{\omega_z}=Q\{-(r_i-\Delta r_i)(2Y_i-W_m+W_t)\\
\qquad+(r_m-\Delta r_m)(2X_m-X_t-D_i)\\
\qquad-(r_t-\Delta r_t)(2X_t-D_i-X_m)\}.
\end{cases} \tag{44}$$

Now, taking inner product of $\dot{\boldsymbol{\Lambda}}=(\dot{\boldsymbol{q}}_i^{\mathrm{T}},\dot{\boldsymbol{q}}_m^{\mathrm{T}},\dot{\boldsymbol{q}}_t^{\mathrm{T}},\dot{\boldsymbol{x}}^{\mathrm{T}},\boldsymbol{\omega}^{\mathrm{T}})^{\mathrm{T}}$ and (35)$\sim$(39) yeilds

$$\frac{\mathrm{d}}{\mathrm{d}t}E = -\sum_{j=i,m,t}(\dot{\boldsymbol{q}}_j^{\mathrm{T}}\boldsymbol{C}_j\dot{\boldsymbol{q}}_j+T_j+\xi\Delta\dot{r}_j^2)\le 0 \tag{45}$$

$$E = K+\Delta P+V\ge 0 \tag{46}$$

$$\begin{aligned}
V &= \frac{Q}{4}\left({I_Y}^2+{I_Z}^2+{M_X}^2+{M_Z}^2+{T_X}^2+{T_Z}^2\right)\\
&\quad+\sum_{j=i,m,t}\frac{1}{2}\hat{\boldsymbol{N}}_j^{\mathrm{T}}\boldsymbol{\Gamma}_{\boldsymbol{N}j}\hat{\boldsymbol{N}}_j\ge 0 \qquad (47)
\end{aligned}$$

$$\Delta P = \sum_{j=i,m,t}\int_0^{\delta r_j}\left\{\bar{f}_j(\Delta r_{d_j}+\xi)-\bar{f}_j(\Delta r_{d_j})\right\}\mathrm{d}\xi, \tag{48}$$

where $\delta r_j=\Delta r_j-\Delta r_{d_j}$ and it is positive definite in δr_j as long as $0\le\Delta r_{d_j}+\delta r_j<r_j$. By choosing adaptive gain $\boldsymbol{\Gamma}_{\boldsymbol{N}j}$ adequately, the scalar function $V\ge 0$ should have a minimum value $V_{\min}$ in a neighborhood of the initial state $\boldsymbol{\Lambda}(0)$ and thereby the scalar function E also has the minimum value $E_{\min}$ in the following way:

$$E_{\min}=K+\Delta P+V-V_{\min}\ge 0. \tag{49}$$

Therefore, from (45) and (49) we obtain the following relation such that

$$\begin{aligned}
&\int_0^\infty\sum_{j=i,m,t}(\dot{\boldsymbol{q}}_j^{\mathrm{T}}\boldsymbol{C}_j\dot{\boldsymbol{q}}_j+T_j+\xi\Delta\dot{r}_j^2)\mathrm{d}t\\
&\qquad\le E_{\min}(0)-E_{\min}(t)\le E_{\min}(0). \qquad (50)
\end{aligned}$$

This means that each joint angular velcity $\dot{\boldsymbol{q}}_j(t)$ is squared integrable over time $t \in (0,\infty)$, that is, $\dot{\boldsymbol{q}}_j(t) \in L^2(0,\infty)$, and by considering six rolling constraints expressed by (12)$\sim$(14), it is possible to see that $\dot{\boldsymbol{x}} \in L^2(0,\infty)$ and $\boldsymbol{\omega} \in L^2(0,\infty)$. Then the velocity vector $\dot{\boldsymbol{\Lambda}}(t)$ becomes uniformly continuous in time t, and finaly we can obtain that $\dot{\boldsymbol{\Lambda}} \to 0$ at $t \to 0$, and also we see $\ddot{\boldsymbol{\Lambda}} \to 0$ as $t \to 0$ [18]. These imply that

$$\boldsymbol{\Delta D_\infty} = (\boldsymbol{\Delta f}^{\mathrm{T}},\ \boldsymbol{\Delta \lambda}^{\mathrm{T}},\ \boldsymbol{\Delta N}^{\mathrm{T}})^{\mathrm{T}} \to \boldsymbol{0} \quad \text{as} \quad t \to \infty, \tag{51}$$
$$\left[\begin{array}{l} \boldsymbol{\Delta f} = (\Delta f_i,\ \Delta f_m,\ \Delta f_t)^{\mathrm{T}} \\ \boldsymbol{\Delta \lambda} = (\boldsymbol{\Delta \lambda}_i^{\mathrm{T}},\ \boldsymbol{\Delta \lambda}_m^{\mathrm{T}},\ \boldsymbol{\Delta \lambda}_t^{\mathrm{T}})^{\mathrm{T}} \\ \boldsymbol{\Delta N} = (\boldsymbol{\Delta N}_i^{\mathrm{T}},\ \boldsymbol{\Delta N}_m^{\mathrm{T}},\ \boldsymbol{\Delta N}_t^{\mathrm{T}})^{\mathrm{T}}. \end{array}\right.$$

Equation (51) means that overall external forces which affect both the fingers and the object converge to zero when time $t \to \infty$. This system is highly redundant and thereby it should carefully treat the convergence of overall state variables. Nevertheless, the convergence could be proven by introducing the concept of "Stability on a manifold" [18] that is omitted here. Eventually, the force/torque equilibrium for the object is satisfied, and the object is thereby immobilized in the dynamical sense.

IV. Numerical Simulation

The parameters used in the simulations are given in Table I. Figure 5 shows the simulation graphics for realization of force/torque equilibrium to immobilize the object by the triple robotic fingers system, and Fig. 6 shows the transient responses of overall external force values $\boldsymbol{\Delta D_\infty}$. We see from Fig. 6 that all componets of $\boldsymbol{\Delta D_\infty}$ converge to zero. It means that any external forces for each finger and the object converge to the equilibrium state eventually. Moreover, Fig. 7 shows the transient responses of overall velocity vector $\dot{\boldsymbol{\Lambda}} = (\dot{\boldsymbol{q}}_j^{\mathrm{T}}, \dot{\boldsymbol{q}}_m^{\mathrm{T}}, \dot{\boldsymbol{q}}_t^{\mathrm{T}}, \dot{\boldsymbol{x}}^{\mathrm{T}}, \boldsymbol{\omega}^{\mathrm{T}})^{\mathrm{T}}$. We can confirm that from Fig. 7, overall velocity vector $\dot{\boldsymbol{\Lambda}}$ converge to zero at the final state. From these results, the force/torque equilibrium to immobilize the object is established in a dynamic manner by using the proposed control scheme.

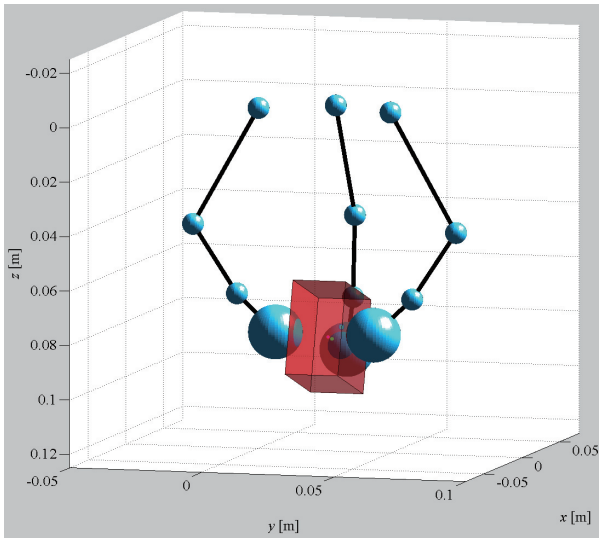

Fig. 5. Simulation graphics for the realization of force/torque equilibrium of the object by the triple robotic fingers system

TABLE I

Parameters for numerical simulations

Triple robotic fingers	
1st link length l_{j1}	0.05 [m]
2nd link length l_{j2}	0.03 [m]
3rd link length l_{j3}	0.02 [m]
1st link mass center lg_{j1}	0.025 [m]
2nd link mass center lg_{j2}	0.015 [m]
3rd link mass center lg_{j3}	0.010 [m]
1st link mass m_{j1}	0.05 [kg]
2nd link mass m_{j2}	0.03 [kg]
3rd link mass m_{j3}	0.02 [kg]
1st link inertia $\boldsymbol{I_{j1}}$	$\mathrm{diag}(1.04, 1.04, 0.06)\times 10^{-5}$ [kg·m^2]
2nd link inertia $\boldsymbol{I_{j2}}$	$\mathrm{diag}(2.25, 2.25, 0.38)\times 10^{-6}$ [kg·m^2]
3rd link inertia $\boldsymbol{I_{j3}}$	$\mathrm{diag}(0.67, 0.67, 0.25)\times 10^{-6}$ [kg·m^2]
Radius of fingertip r_j	0.010 [m]
Stiffness coefficient k_j	3.0×10^5 [N/m^2]
Damping function ξ_j	$500\times(2r_j\Delta r_j - \Delta r_j^2)\pi$ [Ns/m^2]
Damping function η_j	$0.1\times(2r_j\Delta r_j - \Delta r_j^2)\pi$ [Nms]
Object	
Mass m	0.05 [kg]
Height h	0.035 [m]
Width $W_m + W_t$	0.02 [m] ($W_m = W_t = 0.01$ [m])
Depth $D_i + d$	0.035 [m] ($D_i = 0.0175$ [m])
Ineatia $\boldsymbol{I}$	$\mathrm{diag}(0.68, 1.02, 0.68)\times 10^{-5}$ [kg·m^2]
Desired grasping force and each gain	
f_d	1.0 [N]
$\boldsymbol{C}_i,\ \boldsymbol{C}_m$	$\mathrm{diag}(1.5, 1.5, 1.0, 0.8)\times 10^{-3}$
$\boldsymbol{C}_t$	$\mathrm{diag}(1.5, 1.5, 1.5, 1.0, 0.8)\times 10^{-3}$
$\boldsymbol{\Gamma}_{\boldsymbol{N}_i},\ \boldsymbol{\Gamma}_{\boldsymbol{N}_m},\ \boldsymbol{\Gamma}_{\boldsymbol{N}_m}$	$\mathrm{diag}(1.0,\ 1.0,\ 1.0)\times 10^{-4}$
Initial condition	
$\dot{\boldsymbol{q}}_i,\ \dot{\boldsymbol{q}}_m,\ \dot{\boldsymbol{q}}_t$	$\boldsymbol{0}$ [rad/s]
$\boldsymbol{q}_i$	$(0.0, -0.91, -0.83, -0.25)^{\mathrm{T}}$ [rad]
$\boldsymbol{q}_m$	$(0.0, 1.09, 0.95, -0.35)^{\mathrm{T}}$ [rad]
$\boldsymbol{q}_t$	$(0.0, 0.0, 2.05, -0.95, -0.35)^{\mathrm{T}}$ [rad]
$\dot{\boldsymbol{x}}$	$\boldsymbol{0}$ [m/s]
$\boldsymbol{x}$	(0.005,0.025,0.085) [m]
$\boldsymbol{\omega}$	$\boldsymbol{0}$ [rad/s]
$\boldsymbol{R}$	$\boldsymbol{I}_3$
$\hat{\boldsymbol{N}}_i,\ \hat{\boldsymbol{N}}_m, \hat{\boldsymbol{N}}_t$	$\boldsymbol{0}$

V. Conclusion

This paper has proposed a stable object grasping method by modifying the blind grasping control signal in order to utilize it for the triple robotic fingers system. The control signal can be constructed only by using measurement data of finger joint angles and angular velocities, and referring to fingers' kinematics. Its effectiveness in realization of the force/torque equilibrium in object grasping is discussed theoretically with the convergence analysis and confirmed through numerical simulations. In this paper, we treated the specific grasped object that is a rectangular solid. However, our control scheme can be aplicable to other arbitrary polyhedral objects easily. The modeling and analysis for grasping of an arbitrary polyhedral object will be treated in another paper [19]. In the next step of the work, we would consider an arbitrarily shaped 3-dimensional object which is constructed by only smooth curved surfaces.

Acknowledgment

This work was partially supported by Japan Society for the Promotion of Science (JSPS), Grant-in-Aid for Scien-

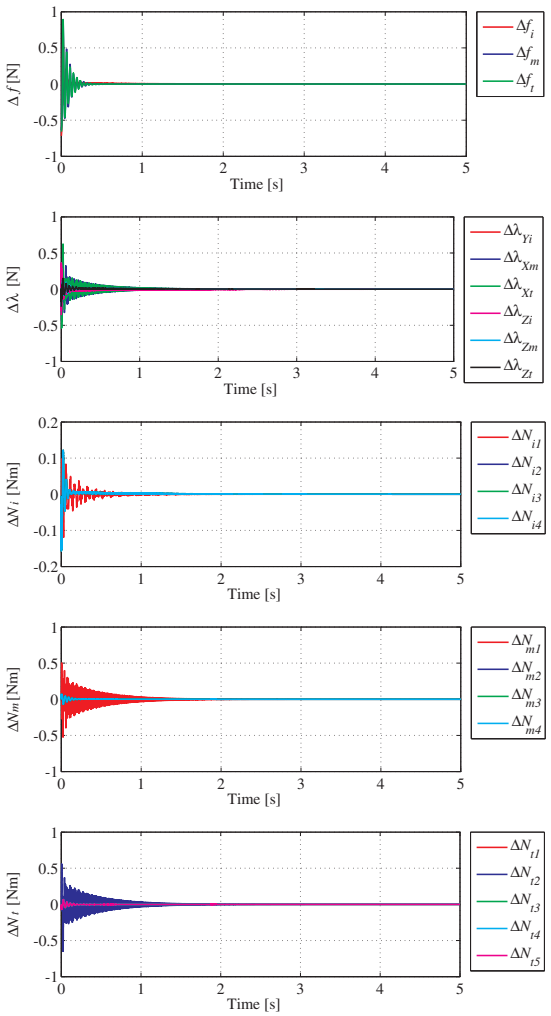

Fig. 6. Force/torque equilibrium realization to immobilize the object by the convergence of external force/torque values $\Delta \boldsymbol{D}_{\infty}$ to zero

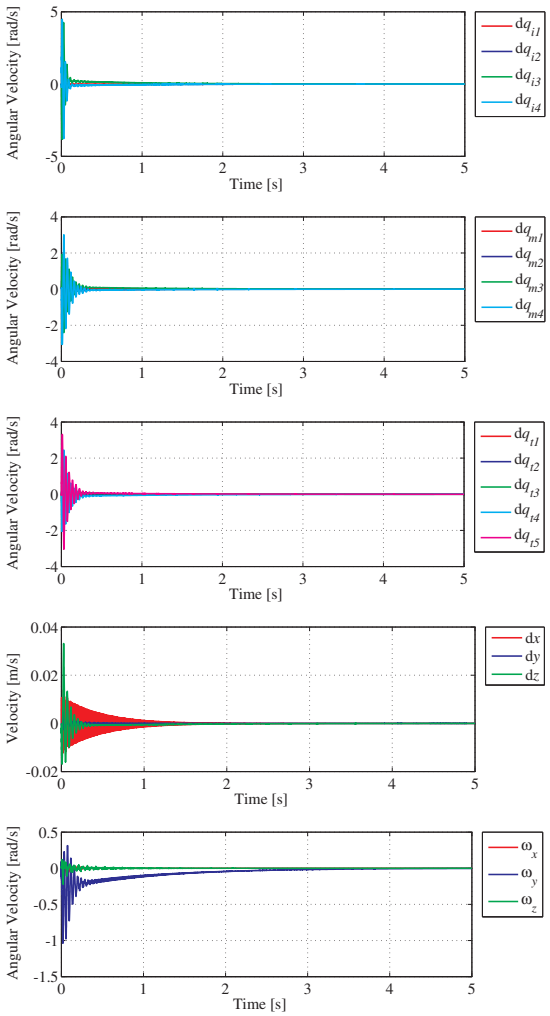

Fig. 7. Transient responses of all velocity vector $\dot{\boldsymbol{\Lambda}}$

tific Research (B) (20360117), and "the Kyushu University Research Superstar Program (SSP)", based on the budget of Kyushu University allocated under President's initiative.

REFERENCES

[1] M.R. Cutkosky, *Grasping and Fine Manipulation*, Kluwer Academic, Dordrecht, Netherlands; 1985.

[2] R.M. Murray, Z. Li and S.S. Sastry, *Mathematical Introduction to Robotic Manipulation*, CRC Press, Boca Raton; 1994.

[3] K.B. Shimoga, "Robot grasp synthesis algorithms: A survey," *Int. J. Robotics Research*, vol. 15, no. 3, pp. 230–266, 1996.

[4] A.M. Okamura, N. Smaby and M.R. Cutkosky, "An overview of dexterous manipulation," *Proc. IEEE Int. Conf. Robott. Automat.*, pp. 255–262, SanFrancisco, CA, 2000.

[5] A. Bicchi, "Hands for dexterous manipulation and robust grasping: A difficult road towards simplicity," *IEEE Trans. Robot. Automat.*, vol. 16, no. 6, pp. 652–662, 2000.

[6] D. Montana, "The kinematics of contact and grasp," *Int. J. Robot. Res.*, vol.7, no. 3, pp. 17–32, 1988.

[7] A. Cole, J. Hauser and S. Sastry, "Kinematics and control of multifingered hands with rolling contacts," *IEEE Trans. Automat. Contr.*, vol. 34, no. 4, pp. 398–404, 1989.

[8] L. Han and J. Trincle, "Dexterous manipulation by rolling and finger gaiting," *Proc. IEEE Int. Conf. Robot. Automat.*, vol. 1, pp. 730–735, 1998.

[9] K. Harada, M. Kaneko, and T. Tsuji, "Rolling based manipulation for multiple objects," *Proc. IEEE Int. Conf. Robot. Automat.*, vol. 4, pp. 3887–3894. 2000.

[10] D. Prattichizzo and A. Bicchi, "Dynamic analysis of mobility and graspability of general manipulation system," *IEEE Trans. Robot. Automat.*, vol. 14, no. 2, pp. 241–258. 1998.

[11] S. Arimoto, P.T.A. Nguyen, H.-Y. Han, and Z. Doulgeri, "Dynamics and control of a set of dual fingers with soft tips," *Robotica*, vol. 18, no. 1, pp. 71–80, 2000.

[12] S. Arimoto, "A differential-geometric approach for 2-D and 3-D object grasping and manipulation," *Annual Review in Control*, Vol. 31, pp. 189–209, 2007.

[13] M. Yoshida, S. Arimoto, and J.-H. Bae, "Blind grasp and manipulation of a rigid object by a pair of robot fingers with soft tips," *Proc. IEEE Int. Conf. Robot. Automat.*, pp. 4707–4714, Roma, Italy, 2007.

[14] J.R. Napier, *Hands,* Princeton Univ. Press; 1993.

[15] J. Czyzowics, I Stojmenovic, J, Urrutia, *Immobilizing a polytope, Lecture Notes Comput. Sci.*, vol. 519, pp. 214–227, Springer; 1991.

[16] M. Yoshida, S. Arimoto and K. Tahara, "Modeling and control of a pair of robot fingers with saddle joint under orderless actuations," *Proc. IEEE Int. Conf. Robot. Automat.*, Kobe, Japan, 2009.

[17] S. Arimoto, *Control Theory of Non-linear Mechanical Systems – A Passivity-based and Circuit-theoretic Approach*, Oxford University Press; 1996.

[18] S. Arimoto, *Control Theory of Multi-fingered Hands –A Modelling and Analytical-Mechanics Approach for Dexterity and Intelligence*, Springer; 2008.

[19] A. Kawamura, K. Tahara, R. Kurazume and T. Hasegawa, "Dynamic grasping for an arbitrary polyhedral object by a multi-fingered hand-arm system," *IEEE/RSJ Int. Conf. Intell. Robot, Syst.*, St. Luis, MO, 2009. (to appear)